

# Distribution-Free Prediction Sets for Regression under Target Shift

Menghan Yi<sup>1</sup>, Yanlin Tang<sup>2</sup>, and Huixia Judy Wang<sup>3,\*</sup>

<sup>1</sup>Department of Biostatistics, University of Michigan, Ann Arbor, MI 48104,  
U.S.A.

<sup>2</sup>KLATASDS-MOE, School of Statistics, East China Normal University,  
Shanghai 200062, China

<sup>3</sup>Department of Statistics, Rice University, Houston, TX 77005, U.S.A.

\*Corresponding author: Huixia Judy Wang, [jw322@rice.edu](mailto:jw322@rice.edu)

October 14, 2025

## Abstract

In real-world applications, the limited availability of labeled outcomes presents significant challenges for statistical inference, due to high collection costs, technical barriers, and other constraints. In this work, we construct efficient conformal prediction sets for new target outcomes by leveraging a source distribution—distinct from the target but related through a distributional shift assumption—that provides abundant labeled data. When the target data are fully unlabeled, our predictions rely solely on the source distribution; when partial labels are available, they are integrated with the source data to improve efficiency. To address the challenges of data non-exchangeability and distribution non-identifiability, we identify the likelihood ratio by matching the covariate distributions of the source and target domains within a finite B-spline space. To accommodate complex

error structures such as asymmetry and multimodality, our method constructs the highest predictive density sets using a novel weight-adjusted conditional density estimator. This estimator models the source conditional density along a quantile process and transforms it—via appropriate weighting adjustments—to approximate the target conditional density. We establish the theoretical properties of the proposed method and evaluate its finite-sample performance through simulation studies and a real-data application to the MIMIC-III clinical database.

**Keywords:** Conformal Prediction, Distribution Shift, Likelihood Ratio, Distribution Matching, Conditional Density Estimation

## 1 Introduction

In many domains—such as clinical medicine and social surveys—collecting complete outcomes from the target distribution  $Q$  is costly or nearly impossible, posing significant challenges to statistical inference. To mitigate this limitation, we leverage a related but distinct source distribution  $P$  that contains abundant labeled outcome data to support the inference process. However, this strategy is not feasible without assuming a relationship between the two distributions. In this paper, we assume a target shift relationship between  $P$  and  $Q$ : the two distributions differ only in the marginal distribution of the outcome  $Y$ , while the conditional distribution of the covariates given the outcome,  $\mathbf{X} \mid Y$ , remains invariant across the two populations. Target shift commonly arises in anti-causal inference settings. For example, in medical diagnosis, we may use symptoms to infer the underlying disease, in which case the distribution of diseases may vary across regions or seasons, whereas the underlying mechanism mapping diseases to symptoms tends to remain stable. It is particularly challenging to infer target distribution quantities under target shift, because the non-exchangeability between training and test data, combined with the scarcity of labeled outcomes, hinders both the identification and correction of the shift. In this paper, we address these challenges by constructing prediction sets for the outcome of a new individual from the target distribution  $Q$  in a regression setting, while ensuring validity even under model misspecification.

Most existing literature on target shift primarily focuses on classification problems in machine learning, following two main lines of research: one based on expectation-maximization (EM) algorithms that maximize the likelihood of unlabeled target samples [Saerens et al., 2002, Chan and Ng, 2005, Alexandari et al., 2020], and the other based on matching moments or distributions between the source and target domains to identify the shift [Plessis and Sugiyama, 2014, Lipton et al., 2018, Azizzadenesheli et al., 2019]. However, existing literature on regression settings with continuous outcomes—which involve infinite-dimensional parameter inference—is relatively limited. Zhang et al. [2013] and Nguyen et al. [2016] tackle the infinite-dimensional challenge by projecting the density function onto a computable function subspace and performing distribution matching within this space. Lee et al. [2025] introduces a flexible estimation approach using the efficient influence function, which remains valid even when the target shift or regression function is misspecified, and applies to both classification and regression settings. However, these methods aim to estimate the unknown components of the target distribution  $Q$ , whereas our goal is fundamentally different—we seek to directly construct prediction sets for a random outcome variable by quantifying uncertainty.

We construct prediction sets for the target variable using conformal prediction [Vovk et al., 2005, Lei et al., 2013, 2018], which measures how well the test point aligns with the training data to form valid prediction sets—without relying on correct model specification. However, under target shift, the exchangeability between the training and test data is violated, rendering standard conformal prediction invalid. Several recent studies have investigated conformal prediction under distribution shift. For example, Gibbs and Candès [2021, 2024] proposed a framework for handling arbitrary time-varying distribution shifts in an online setting, where the confidence level is dynamically adjusted to ensure valid prediction intervals over time. Barber et al. [2023] mitigate the coverage loss caused by non-exchangeability by assigning fixed weights to samples. Cauchois et al. [2024] address arbitrary distribution shifts by characterizing worst-case quantiles within an  $f$ -divergence ball centered at the training distribution. Although these methods provide valid predictions under arbitrary distribution shifts with unknown form, they tend to be conservative in our target shift setting. To this

end, we adopt a likelihood ratio-based weighted conformal prediction approach [Tibshirani et al., 2019, Lei and Candès, 2021, Candes et al., 2023], which leverages knowledge of the distribution shift to more precisely correct for non-exchangeability and to enable more efficient predictive inference. However, its validity relies on access to the true likelihood ratio of the distribution shift, which is particularly challenging to identify in the absence of labeled target data.

In this work, we propose Conformal Prediction Under Target Shift (CPUTS), which addresses distribution non-identifiability and data non-exchangeability by identifying a likelihood-ratio weight through covariate distribution matching that leverages target-domain information. Our method offers several key contributions and innovations. First, we propose a flexible uncertainty quantification framework for regression under target shift, which is designed to address two practical scenarios: (i) when  $Q$  contains no labeled data, predictions are generated by leveraging labeled data from the source distribution  $P$ ; and (ii) when limited labels are available in  $Q$ , they are utilized together with information from  $P$  to enhance predictive efficiency. Our work provides a complementary and more comprehensive counterpart to Podkopaev and Ramdas [2021], which studied a classification task under an unlabeled target scenario. Second, we provide an approach to estimate the label likelihood ratio by projecting it onto a B-spline basis space, enabling an effective match between the reweighted source distribution and the target distribution. This estimator is supported by theoretical guarantees and offers greater flexibility in capturing the local characteristics of target shift in practice than the methods proposed in Zhang et al. [2013] and Nguyen et al. [2016]. Finally, to improve efficiency, we construct the prediction sets using the target conditional density. This results in more compact prediction sets than those produced by standard methods [Vovk et al., 2005, Tibshirani et al., 2019], particularly when the conditional distribution is asymmetric, heteroscedastic, or multimodal. However, estimating the conditional density is highly challenging in the absence of target labels. To address this issue, we propose a weighted adjustment estimator that first estimates the conditional density under  $P$  using a quantile process-based approach, and then applies a target shift correction to recover the

corresponding density under  $Q$ .

The remainder of the article is structured as follows. Section 2 introduces the proposed method, including the problem setup, motivation, and the CPUTS procedure for both unlabeled and labeled target scenarios. Theoretical properties are discussed in Section 3. Section 4 provides empirical results from simulation studies. In Section 5, we illustrate the application of our method using the MIMIC-III database. Finally, Section 6 concludes the article with a discussion. Additional technical details are provided in the supplementary materials.

## 2 Proposed Method

### 2.1 Setup and Motivation

Let  $Y$  denote the univariate response variable of interest and  $\mathbf{X} \in \mathbb{R}^p$  the corresponding covariate vector, jointly drawn from either the source distribution  $P(\mathbf{x}, y)$  or the target distribution  $Q(\mathbf{x}, y)$ . The source  $P(\mathbf{x}, y)$  provides abundant labeled data, denoted as  $\{(\mathbf{X}_i^P, Y_i^P)\}_{i=1}^{n_P}$ , whereas the target  $Q(\mathbf{x}, y)$  typically includes only covariates, denoted as  $\{\mathbf{X}_i^Q\}_{i=1}^{n_Q}$ , with few or no corresponding labels. Given a new individual from the target distribution with observed covariates  $\mathbf{X}_{n+1}^Q$  and an unobserved response  $Y_{n+1}^Q$ , our goal is to construct a covariate-dependent prediction set  $\widehat{C}(\mathbf{X}_{n+1}^Q; \alpha)$  for the response, such that the following coverage guarantee holds:

$$\mathbb{P} \left\{ Y_{n+1}^Q \in \widehat{C}(\mathbf{X}_{n+1}^Q; \alpha) \right\} \geq 1 - \alpha, \quad (1)$$

where  $\alpha \in (0, 1)$  is a user-specified miscoverage level, and the probability  $\mathbb{P}$  accounts for all sources of randomness in the data.

Predicting  $Y_{n+1}^Q$  is particularly challenging due to the lack of labeled data. To address this, we aim to leverage labeled source data for prediction, which requires an underlying relationship between the source and target distributions. In our work, we assume that this relationship follows the target shift assumption,

$$p(y) \neq q(y) \quad \text{but} \quad p(\mathbf{x} \mid y) = q(\mathbf{x} \mid y),$$

a setting commonly encountered in real-world applications involving inverse inference. In this setting, existing work [Nguyen et al., 2016, Lee et al., 2025] typically focuses on inferring specific parameters or functionals of  $Q(\mathbf{x}, y)$ , whereas our goal is to directly construct a prediction interval for  $Y_{n+1}^Q$  by quantifying uncertainty. To this end, we leverage conformal prediction [Lei et al., 2013, 2018] to construct distribution-free prediction sets that quantify predictive uncertainty by assessing how well new test points conform to the observed data. However, its coverage guarantee relies on the exchangeability assumption, which does not hold in our target shift setting. Moreover, limited or missing labels in the target distribution pose significant challenges for identifying the underlying distribution.

In this work, we propose a method called Conformal Prediction Under Target Shift (CPUTS), which addresses the challenges of non-exchangeability and distributional non-identifiability to construct prediction sets that satisfy the coverage guarantee (1). Our method is designed to address two practical scenarios. In **Scenario 1**, where no labels are available from target  $Q(\mathbf{x}, y)$ , CPUTS constructs predictions solely based on labeled data from the source  $P(\mathbf{x}, y)$ . In **Scenario 2**, where a small portion of target samples is labeled, CPUTS primarily utilizes the labeled data from  $Q(\mathbf{x}, y)$  to construct predictions, while incorporating  $P(\mathbf{x}, y)$  data to enhance prediction efficiency. Details of the CPUTS methods for Scenario 1 and Scenario 2 are provided in Sections 2.2 and 2.3, respectively.

## 2.2 CPUTS on Unlabeled Data

The idea of CPUTS is to construct the prediction set by including all plausible values  $y$  of  $Y_{n+1}^Q$  that cannot be rejected by a level- $\alpha$  test of the null hypothesis  $H_0 : Y_{n+1}^Q = y$ . To test the hypothesis, we construct a nonconformity score to evaluate the conformity of the test point  $y$  with the trained model and determine whether to reject the hypothesis based on its rank. However, under distribution shift, the distribution of this rank is no longer uniform and therefore fails to reflect the true conformal level.

Although existing methods [Tibshirani et al., 2019, Lei and Candès, 2021, Candes et al., 2023] can correct for covariate shift by reweighting samples using the density ratio between the

source and target domains, this approach is impractical in our setting, as neither the density ratio nor the nonconformity score can be identified without labeled target data. To address this issue, we propose a method that approximates the density ratio by matching the marginal covariate distributions of the source and target domains in a sieve-based projection space. Under the target shift assumption, this approach enables flexible and effective correction for distribution mismatch and supports accurate estimation of the nonconformity score. Our method includes four main steps, and the data overview is shown in Figure 1.

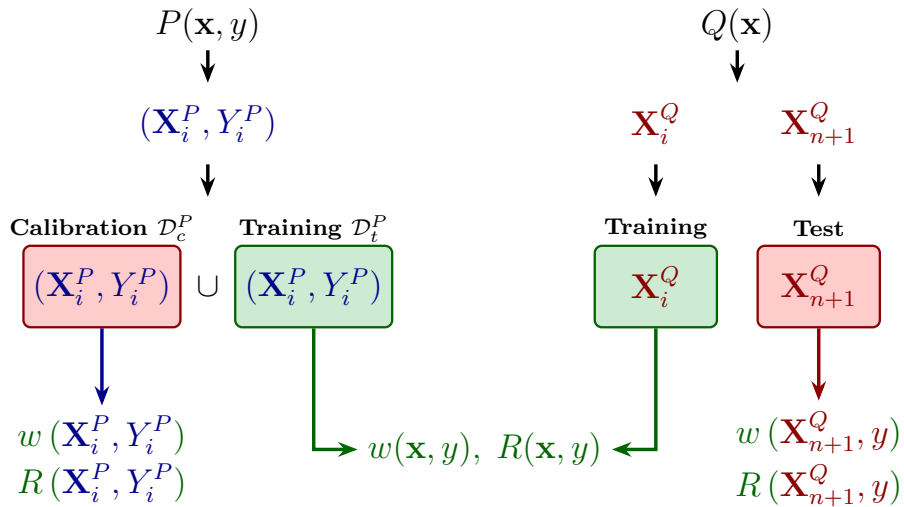


Figure 1: Data sources used for  $p$ -value computation in CPUTS under Scenario 1.

**Step 1: Data Splitting.** Recall that the available datasets are as follows:

$$\{(\mathbf{X}_i^P, Y_i^P)\}_{i=1}^{n_P} \stackrel{\text{i.i.d.}}{\sim} P(\mathbf{x}, y), \quad \{\mathbf{X}_i^Q\}_{i=1}^{n_Q} \cup \mathbf{X}_{n+1}^Q \stackrel{\text{i.i.d.}}{\sim} Q(\mathbf{x}, y).$$

We split the labeled  $P$  data into two disjoint subsets: a training set  $\mathcal{D}_t^P$  and a calibration set  $\mathcal{D}_c^P$ . The set  $\mathcal{D}_t^P$ , together with the unlabeled  $Q$  data, is used to estimate the target shift and fit the nonconformity score function, while  $\mathcal{D}_c^P$  is used to compute and compare nonconformity scores for the test point.

**Step 2: Nonconformity Score.** Define a nonconformity score function  $R(\mathbf{x}, y) : \mathcal{X} \times \mathcal{Y} \rightarrow \mathbb{R}$  that quantifies the degree of deviation between a test point  $(\mathbf{x}, y)$  and the trained model, where a larger score indicates greater deviation. This function can be chosen flexibly

without affecting the coverage guarantee. In CPUTS, we set

$$R(\mathbf{x}, y; \hat{q}) = -\hat{q}(y \mid \mathbf{x}),$$

where  $\hat{q}(y \mid \mathbf{x})$  denotes the estimated conditional density of  $y$  given  $\mathbf{x}$  under the target distribution  $Q$ . Using the conditional density as the nonconformity score captures the full structure of the target distribution and yields the highest predictive density sets [Izbicki et al., 2022] that can accommodate heteroscedasticity, asymmetry, and multimodal residuals. Compared to standard residual-based scores [Shafer and Vovk, 2008, Lei et al., 2018, Tibshirani et al., 2019], our choice yields smaller and more informative prediction sets. However, conditional density estimation is particularly challenging in our setting, as no true  $Y$  values are available from the target distribution. To address this challenge, we propose a bias-corrected method that first estimates the source conditional density and then adjusts it to recover the target version based on their distributional relationship; see Section 2.2.2.

**Step 3: Evaluate the nonconformity of the test point.** We compare the nonconformity score of the test point  $y$  with those from the calibration set  $\mathcal{D}_c^P$ . Since these scores are derived from different distributions and are therefore not directly comparable, we apply a density ratio weight

$$w(\mathbf{x}, y) = \frac{q(\mathbf{x}, y)}{p(\mathbf{x}, y)} \quad (2)$$

to restore comparability and adjust the ranking. This yields a weighted  $p$ -value that quantifies the percentile rank of the test point's nonconformity score:

$$p(y) = \sum_{i \in \mathcal{D}_c^P \cup \{n+1\}} \varpi_i(y) \mathbb{I}\{R(\mathbf{X}_i^P, Y_i^P) \geq R(\mathbf{X}_{n+1}^Q, y)\}, \quad (3)$$

where the weights  $\varpi_i(y)$  are normalized based on the density ratio function (2):

$$\begin{aligned} \varpi_i(y) &= \frac{w(\mathbf{X}_i^P, Y_i^P)}{\sum_{j \in \mathcal{D}_c^P} w(\mathbf{X}_j^P, Y_j^P) + w(\mathbf{X}_{n+1}^Q, y)}, \quad i \in \mathcal{D}_c^P, \\ \varpi_{n+1}(y) &= \frac{w(\mathbf{X}_{n+1}^Q, y)}{\sum_{j \in \mathcal{D}_c^P} w(\mathbf{X}_j^P, Y_j^P) + w(\mathbf{X}_{n+1}^Q, y)}. \end{aligned}$$

Estimating the weight function is also highly challenging due to the lack of data required to identify  $q(\mathbf{x}, y)$ . To address this, we propose a distribution-matching approach that avoids explicit estimation of  $q(\mathbf{x}, y)$  and instead directly recovers the ratio  $w(\mathbf{x}, y)$  by aligning the covariate distributions from the source and target domains. See Section 2.2.1 for details. An overview of the  $p$ -value computation process is shown in Figure 1.

**Step 4: Construct the prediction set.** We construct the prediction set by including candidate values of  $y$  with higher conformity to the trained model, as indicated by larger  $p$ -values:  $\widehat{C}(\mathbf{X}_{n+1}^Q; \alpha) = \{y : p(y) > \alpha\}$ .

### 2.2.1 Weight Estimation

Under the target shift assumption  $q(\mathbf{x}|y) = p(\mathbf{x}|y)$ , the density ratio simplifies to

$$w(\mathbf{x}, y) = \frac{q(\mathbf{x}, y)}{p(\mathbf{x}, y)} = \frac{q(y)}{p(y)} := w(y).$$

This expression indicates that the density ratio primarily depends on the marginal distribution  $q(y)$ , which is not identifiable without labeled target data. To overcome this challenge, we adopt the distribution-matching approach [Zhang et al., 2013, Nguyen et al., 2016, Guo et al., 2020], which directly estimates  $w(y)$  by aligning the observed covariate information in the target domain with that implied by the source distribution.

Define the reweighted distribution  $q_w(\mathbf{x}) := \int w(y)p(\mathbf{x}, y)dy$  with respect to the source distribution. Under the target shift assumption, if the weight function takes its true form  $w(y) = q(y)/p(y)$ , then  $q_w(\mathbf{x}) = q(\mathbf{x})$ . Therefore,  $w(y)$  can be estimated by minimizing the discrepancy between  $q_w(\mathbf{x})$  and  $q(\mathbf{x})$ , subject to the non-negativity constraint  $w(y) \geq 0$  and the normalization constraint  $\int w(y)p(y)dy = 1$ . However, this minimization problem is infinite-dimensional and requires estimating the unknown densities  $q(\mathbf{x})$  and  $p(\mathbf{x}, y)$ , which may be high-dimensional. To address these challenges, we approximate both the weight

function  $w(y)$  and the density difference  $q(\mathbf{x}) - q_w(\mathbf{x})$  using basis expansions:

$$w(y) \approx \sum_{j=1}^{J_n} \alpha_j B_j(y) = \boldsymbol{\alpha}^\top \mathbf{B}(y), \quad q(\mathbf{x}) - q_w(\mathbf{x}) \approx \sum_{k=1}^{K_n} \beta_k \psi_k(\mathbf{x}) = \boldsymbol{\beta}^\top \boldsymbol{\psi}(\mathbf{x}), \quad (4)$$

where  $\mathbf{B}(y) = [B_1(y), \dots, B_{J_n}(y)]^\top$  and  $\boldsymbol{\psi}(\mathbf{x}) = [\psi_1(\mathbf{x}), \dots, \psi_{K_n}(\mathbf{x})]^\top$  are vectors of  $J_n$  and  $K_n$  basis functions, respectively, and  $\boldsymbol{\alpha} \in \mathbb{R}^{J_n}$ ,  $\boldsymbol{\beta} \in \mathbb{R}^{K_n}$  are the corresponding coefficient vectors. We employ univariate B-spline basis functions of degree  $d$  [Schumaker, 2007], denoted by  $B_j(y) := B_{j,d}(y)$ , for the response space, and Gaussian radial basis functions [Buhmann, 2000], defined as  $\psi_k(\mathbf{x}) = \exp\{-\|\mathbf{x} - \boldsymbol{\mu}_k\|^2/(2\sigma_k^2)\}$ , for the covariate space, where  $\boldsymbol{\mu}_k$  and  $\sigma_k$  denote the center and bandwidth, respectively.

To estimate  $\boldsymbol{\beta}$  in (4), we minimize the integrated squared error between the true function and its approximation via the basis expansion:

$$\int [\boldsymbol{\beta}^\top \boldsymbol{\psi}(\mathbf{x}) - \{q(\mathbf{x}) - q_w(\mathbf{x})\}]^2 d\mathbf{x} = \boldsymbol{\beta}^\top \mathbf{U} \boldsymbol{\beta} - 2\boldsymbol{\beta}^\top (\mathbf{V} \boldsymbol{\alpha} - \mathbf{u}) + C,$$

where  $\mathbf{U} = \int \boldsymbol{\psi}(\mathbf{x}) \boldsymbol{\psi}^\top(\mathbf{x}) d\mathbf{x}$ ,  $\mathbf{V} = \mathbb{E}_{(\mathbf{x}, Y) \sim p(\mathbf{x}, y)} [\boldsymbol{\psi}(\mathbf{X}) \mathbf{B}^\top(Y)]$ ,  $\mathbf{u} = \mathbb{E}_{\mathbf{X} \sim q(\mathbf{x})} [\boldsymbol{\psi}(\mathbf{X})]$ , and the term  $C$  is a constant independent of  $\boldsymbol{\beta}$ . The equality holds because  $q_w(\mathbf{x})$  is approximated by  $\boldsymbol{\alpha}^\top \int \mathbf{B}(y) p(\mathbf{x}, y) dy$ . Therefore, the closed-form solution is given by

$$\hat{\boldsymbol{\beta}}(\boldsymbol{\alpha}) = (\mathbf{U} + \delta_n \mathbf{I})^{-1} (\hat{\mathbf{V}} \boldsymbol{\alpha} - \hat{\mathbf{u}}),$$

where  $\hat{\mathbf{V}} = \frac{1}{|\mathcal{D}_t^P|} \sum_{i \in \mathcal{D}_t^P} \boldsymbol{\psi}(\mathbf{X}_i^P) \mathbf{B}^\top(Y_i^P)$ ,  $\hat{\mathbf{u}} = \frac{1}{n_Q} \sum_{i=1}^{n_Q} \boldsymbol{\psi}(\mathbf{X}_i^Q)$ , and  $\delta_n$  is a regularization parameter introduced to enhance numerical stability and prevent overfitting. Finally,  $\boldsymbol{\alpha}$  is estimated by minimizing the integrated squared error  $\int \{q(\mathbf{x}) - q_w(\mathbf{x})\}^2 d\mathbf{x}$ , whose empirical counterpart is  $\hat{\boldsymbol{\beta}}(\boldsymbol{\alpha})^\top \mathbf{U} \hat{\boldsymbol{\beta}}(\boldsymbol{\alpha})$ , leading to the following optimization problem:

$$\hat{\boldsymbol{\alpha}} = \underset{\boldsymbol{\alpha}}{\operatorname{argmin}} \left[ \boldsymbol{\alpha}^\top \hat{\mathbf{V}}^\top (\mathbf{U} + \delta_n \mathbf{I})^{-1} \hat{\mathbf{V}} \boldsymbol{\alpha} - 2\hat{\mathbf{u}}^\top (\mathbf{U} + \delta_n \mathbf{I})^{-1} \hat{\mathbf{V}} \boldsymbol{\alpha} + \rho_n \boldsymbol{\alpha}^\top \boldsymbol{\alpha} \right],$$

subject to the constraints  $\boldsymbol{\alpha}^\top \mathbf{B}(y) \geq 0$  and  $\boldsymbol{\alpha}^\top \mathbb{E}_{Y \sim p(y)} [\mathbf{B}(Y)] = 1$ , where  $\rho_n$  is a regularization parameter. Hence, the estimated weight function is given by  $\hat{w}(y) = \hat{\boldsymbol{\alpha}}^\top \mathbf{B}(y)$ .

In our approach, we employ B-spline basis functions to flexibly model the complex shape of  $w(y)$  arising from various types of distribution shift. Compared to global basis functions [Zhang et al., 2013, Nguyen et al., 2016], the compact support of B-splines allows for more precise local control, offering a distinct advantage in modeling localized variation in practice. Moreover, the use of Gaussian radial basis functions facilitates computation over the covariate space, as the  $L^2$  inner product matrix  $\mathbf{U} = \int \psi(\mathbf{x})\psi^\top(\mathbf{x})d\mathbf{x}$  admits a closed-form expression, eliminating the need for numerical integration.

### 2.2.2 Conditional Density Estimation

To estimate the target conditional density, a natural and intuitive strategy is to first estimate the source density using the labeled data and then adjust it based on the relationship between the two distributions. Specifically, we construct the following reweighted density estimator via Bayes' rule:

$$\hat{q}(y | \mathbf{x}) := \frac{\hat{p}(y | \mathbf{x})\hat{w}(y)}{\int \hat{p}(y | \mathbf{x})\hat{w}(y)dy}, \quad (5)$$

where  $\hat{w}(y)$  denotes the estimated density ratio  $q(y)/p(y)$  obtained in Section 2.2.1, and  $\hat{p}(y | \mathbf{x})$  is the conditional density under source distribution  $P$ .

Standard methods for estimating the conditional density  $\hat{p}$ —including kernel and  $k$ -nearest neighbors techniques—are fundamentally limited by the curse of dimensionality [Hastie et al., 2009]. To address this challenge, we adopt a semi-parametric approach that reconstructs the conditional density through a quantile process induced by a working conditional quantile model. Importantly, the validity of the proposed CPUTS procedure does not rely on the correct specification of this model. Let  $\xi_P(\tau | \mathbf{x})$  denote the  $\tau$ -th conditional quantile of  $Y$  given  $\mathbf{x}$  under distribution  $P$ . For a continuous distribution, the conditional density  $p(y | \mathbf{x})$ , evaluated at the point  $y = \xi_P(\tau | \mathbf{x})$ , satisfies  $p(\xi_P(\tau | \mathbf{x}) | \mathbf{x}) = \{d\xi_P(\tau | \mathbf{x})/d\tau\}^{-1}$ . Therefore, we construct the quotient estimator [Siddiqui, 1960] as

$$\hat{p}(\hat{\xi}_P(\tau | \mathbf{x}) | \mathbf{x}) = \frac{2h_n}{\hat{\xi}_P(\tau + h_n | \mathbf{x}) - \hat{\xi}_P(\tau - h_n | \mathbf{x})}, \quad (6)$$

where  $h_n$  is a bandwidth that shrinks to zero as  $n \rightarrow \infty$  and  $\hat{\xi}_P(\tau \mid \mathbf{x})$  denotes the estimated conditional  $\tau$ -quantile under the source distribution  $P$ . The quantile estimates can be obtained using any appropriate quantile regression method under a working model, such as linear quantile regression [Koenker, 2005] or quantile random forests [Athey et al., 2019]. To estimate the full conditional density  $\hat{p}(y \mid \mathbf{x})$ , we first specify a set of quantile levels  $\{\tau_1^P, \dots, \tau_{\kappa^P}^P\}$  and compute density estimates at the corresponding estimated quantile values  $\{\hat{\xi}_P(\tau_1^P \mid \mathbf{x}), \dots, \hat{\xi}_P(\tau_{\kappa^P}^P \mid \mathbf{x})\}$  using equation (6). These pointwise estimates are then interpolated—e.g., linearly or using splines—to approximate  $\hat{p}(y \mid \mathbf{x})$  for any value of  $y$ .

## 2.3 CPUTS on Labeled Data

Suppose we have labeled samples from the source distribution and partially labeled samples from the target distribution, where only the first  $n_0$  out of  $n_Q$  target samples have labels:

$$\{(\mathbf{X}_i^P, Y_i^P)\}_{i=1}^{n_P} \stackrel{\text{i.i.d.}}{\sim} P(\mathbf{x}, y), \quad \{(\mathbf{X}_i^Q, Y_i^Q)\}_{i=1}^{n_0} \cup \{\mathbf{X}_j^Q\}_{j=n_0+1}^{n_Q} \cup \mathbf{X}_{n+1}^Q \stackrel{\text{i.i.d.}}{\sim} Q(\mathbf{x}, y).$$

In this setting, a natural strategy is to construct the prediction primarily based on the  $Q$  data, while incorporating the  $P$  data as auxiliary information to enhance predictive efficiency. Since the predictive efficiency of conformal prediction heavily relies on the accurate estimation of nonconformity scores [Dunn et al., 2023, Hu and Lei, 2024], we leverage all the labeled  $Q$  data for model training to reduce the length of the resulting prediction sets, while incorporating information from  $P$  to assist in computing the  $p$ -values. This splitting strategy was shown in our preliminary study to provide greater improvements in efficiency compared to other data-splitting approaches.

Our CPUTS method follows a procedure similar to that in Scenario 1, using the  $p$ -value defined in (3) to construct the prediction region. The only difference lies in the use of a more informative nonconformity score:

$$R(\mathbf{x}, y) = (1 - K)R_1(\mathbf{x}, y) + KR_2(\mathbf{x}, y),$$

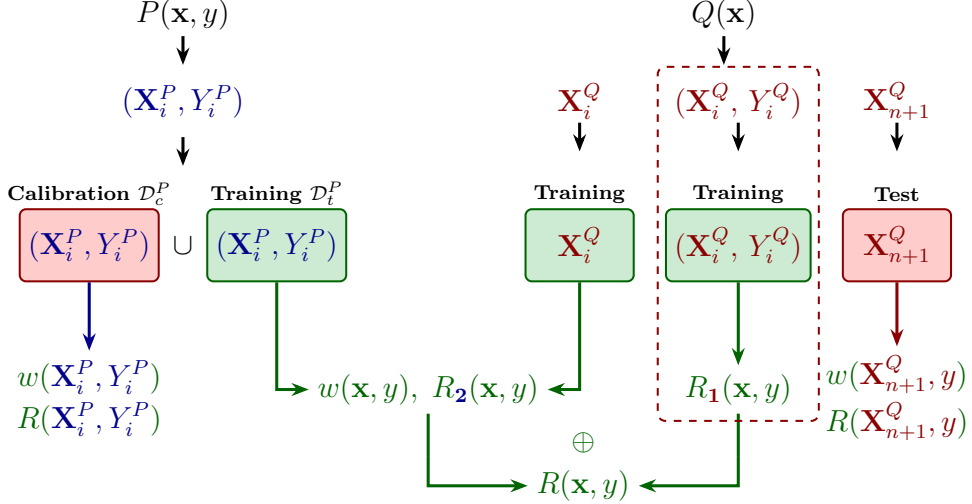


Figure 2: Data sources used for  $p$ -value computation in CPUTS under Scenario 2.

where  $R_1(\mathbf{x}, y)$  is trained on labeled data from  $Q$ ,  $R_2(\mathbf{x}, y)$  is the same score as in Scenario 1, fitted on labeled data from  $P$  combined with unlabeled covariates from  $Q$ , and  $K \in [0, 1]$  controls their relative contributions. Let  $\sigma_1^2 = \text{Var}(R_1)$  and  $\sigma_2^2 = \text{Var}(R_2)$  denote their variances with respect to the training data. Since  $R_1$  and  $R_2$  are independent, for any  $K$ , the variance of the combined nonconformity score  $R$  is  $\text{Var}(R) = (1 - K)^2\sigma_1^2 + K^2\sigma_2^2$ . By minimizing this variance, the optimal  $K$  is given by  $K^* = \sigma_1^2/(\sigma_1^2 + \sigma_2^2)$ . Since the variance of an estimator typically decreases with larger sample sizes (i.e.,  $\sigma_1^2 \propto 1/n_0$  and  $\sigma_2^2 \propto 1/|\mathcal{D}_t^P|$ ), we approximate the optimal weight  $K^*$  by  $K = |\mathcal{D}_t^P|/(n_0 + |\mathcal{D}_t^P|)$ , which assigns weights proportional to the available sample sizes, reflecting the inverse-variance weighting in a practical and stable manner.

To construct  $R_1(\mathbf{x}, y) = -\hat{q}(y \mid \mathbf{x})$  based on the  $Q$  data, we directly estimate  $\hat{q}(y \mid \mathbf{x})$  using the quotient estimator on its labeled samples. Similar to (6), the conditional density at  $\xi_Q(\tau \mid \mathbf{x})$ —the  $\tau$ -th conditional quantile of  $Y$  given  $\mathbf{x}$  under distribution  $Q$ —can be estimated as:

$$\hat{q}\{\hat{\xi}_Q(\tau \mid \mathbf{x}) \mid \mathbf{x}\} = \frac{2h_n}{\hat{\xi}_Q(\tau + h_n \mid \mathbf{x}) - \hat{\xi}_Q(\tau - h_n \mid \mathbf{x})},$$

where  $h_n$  is a bandwidth tending to zero as  $n \rightarrow \infty$ , and  $\hat{\xi}_Q(\tau \mid \mathbf{x})$  is the estimated  $\tau$ -th conditional quantile. Therefore, we can estimate  $\hat{q}(y \mid \mathbf{x})$  at any point  $y$  by interpolating the

estimated conditional density values along the quantile process  $\{\widehat{\xi}_Q(\tau_1^Q | \mathbf{x}), \dots, \widehat{\xi}_Q(\tau_{\kappa^Q}^Q | \mathbf{x})\}$ , where  $\{\tau_1^Q, \dots, \tau_{\kappa^Q}^Q\}$  is a prespecified set of quantile levels. Moreover, the score  $R_2(\mathbf{x}, y) = -\widehat{q}(y | \mathbf{x})$ , constructed from the  $P$  data, corresponds to the estimate used in Scenario 1, as specified in equation (5). The overall procedure is illustrated in Figure 2.

### 3 Theoretical Properties

In this section, we first establish that the proposed CPUTS method guarantees coverage under a single condition—that the weights are finite almost surely—where the coverage accuracy depends on the precision of the weight estimation. The asymptotic properties of the weight estimator are presented later under standard regularity conditions.

**Assumption 1** *The likelihood-ratio weight  $w(y) = q(y)/p(y)$  is finite almost surely under the target distribution  $Q$ ; that is,  $\mathbb{P}_{Y \sim Q}\{w(Y) < \infty\} = 1$ .*

Assumption 1 is equivalent to requiring that the target distribution  $Q$  is absolutely continuous with respect to the source distribution  $P$ ,  $Q \ll P$ , which in turn implies that the support of  $Q$  is contained in the support of  $P$ .

**Theorem 1** *Under Assumption 1, suppose the estimated weight function  $\widehat{w}$  is integrable under  $P$ , i.e.  $\mathbb{E}_{Y \sim P}\{\widehat{w}(Y)\} < \infty$ . Then, for any  $\alpha \in (0, 1)$ , the CPUTS method satisfies*

$$\mathbb{P}\{Y_{n+1} \in \widehat{C}(\mathbf{X}_{n+1}; \alpha)\} \geq 1 - \alpha - \frac{1}{2}\mathbb{E}_{Y \sim P}|\widehat{w}(Y) - w(Y)|.$$

The proof of Theorem 1 is provided in the supplementary material. Theorem 1 demonstrates that when the target shift weight is known, the CPUTS method guarantees an exact coverage lower bound of  $1 - \alpha$ . Alternatively, when the weight is unknown, the coverage bound includes an additional error term that depends on the accuracy of the weight estimation. With our proposed estimator, this error becomes asymptotically negligible. In Theorem 2, we show that under standard regularity conditions, the estimated weight function  $\widehat{w}(\cdot)$  converges to the true weight  $w(\cdot)$  at a rate of  $O(n^{-\gamma})$  for some  $\gamma > 0$ .

The CPUTS method satisfies the coverage lower bound established in Theorem 1 for both the unlabeled (Section 2.2) and labeled (Section 2.3) target scenarios. In the labeled scenario, the additional labeled target data do not improve the theoretical coverage bound but can help shorten the prediction intervals while maintaining reasonable coverage. This is because our data-splitting strategy allocates the target data entirely to improving the efficiency of nonconformity score estimation.

Before presenting the asymptotic properties of the weight estimator, we introduce the necessary regularity conditions.

**Assumption 2 (Weight Function Approximation)** *The weight function  $w(y)$  belongs to the Sobolev space  $W^{r,2}([a, b])$  with  $r > 1/2$ . We approximate  $w(y)$  using B-spline basis functions  $\{B_{j,d}(y)\}_{j=1}^{J_n}$  of degree  $d$ , and impose the following conditions: (a) The spline degree satisfies  $d \geq \lceil r \rceil$ ; (b) There exists a constant  $C_B > 0$  such that  $\max_{1 \leq j \leq J_n} \|B_{j,d}\|_{\psi_2} \leq C_B$ , where  $\|\cdot\|_{\psi_2}$  denotes the sub-Gaussian Orlicz norm; (c) The knot sequence  $\{t_j\}$  is quasi-uniform, i.e., there exists a constant  $C > 0$  such that  $\max_j (t_{j+1} - t_j) \leq C \min_j (t_{j+1} - t_j)$ .*

**Assumption 3 (Density Difference Approximation)** *The density difference function  $t(\mathbf{x}) := q(\mathbf{x}) - q_w(\mathbf{x})$  belongs to the Sobolev space  $W^{s,2}(\Omega)$  with  $\Omega \subset \mathbb{R}^p$ . We approximate  $t(\mathbf{x})$  using Gaussian radial basis functions  $\{\psi_k(\mathbf{x})\}_{k=1}^{K_n}$  and impose the following conditions: (a) The smoothness parameter satisfies  $s > p/2$ ; (b) There exists a constant  $C_\psi > 0$  such that  $\max_{1 \leq k \leq K_n} \|\psi_k\|_{\psi_2} \leq C_\psi$ ; (c) The fill distance  $h_{K_n} := \sup_{\mathbf{x} \in \Omega} \min_k \|\mathbf{x} - \boldsymbol{\mu}_k\|$  satisfies  $h_{K_n} \asymp K_n^{-1/p}$ , and the widths satisfy  $\sigma_k \asymp h_{K_n}$ .*

**Assumption 4 (Sieve Gram matrix)** *Let  $\mathbf{G}_J := \int \mathbf{B}(y) \mathbf{B}^\top(y) dy$ . There exist constants  $c_{\min}, c_{\max} > 0$  such that  $c_{\min} J_n^{-1} \leq \lambda_{\min}(\mathbf{G}_J) \leq \lambda_{\max}(\mathbf{G}_J) \leq c_{\max} J_n^{-1}$ .*

**Assumption 5 (Dimensionality versus sample size)** *The sieve dimensions  $(J_n, K_n)$  grow with the sample sizes  $n_P$  and  $n_Q$ , and satisfy  $K_n J_n \log n_P = o(n_P)$ ,  $K_n \log n_Q = o(n_Q)$ .*

**Assumption 6 (Non-singularity)** *Let the ridge parameters  $\delta_n, \rho_n \rightarrow 0$ . Suppose there exist constants  $C_0, C_1, C'_0, C'_1$  such that  $\lambda_{\min}(\mathbf{U}) \geq C'_0 n_P^{-1/2}$ ,  $\lambda_{\min}(\mathbf{V}^\top \mathbf{U}^{-1} \mathbf{V}) \geq C'_1 n_Q^{-1/2}$ ,  $\lambda_{\min}(\mathbf{U} + \delta_n \mathbf{I}) \geq C_0 n_P^{-1/2}$ , and  $\lambda_{\min}(\mathbf{V}^\top (\mathbf{U} + \delta_n \mathbf{I})^{-1} \mathbf{V} + \rho_n \mathbf{I}) \geq C_1 n_Q^{-1/2}$ .*

Assumptions 2 and 3 require that  $w(y)$  and  $t(\mathbf{x})$  lie in sufficiently smooth Sobolev spaces and be approximated using B-spline and Gaussian radial basis functions of appropriate orders, respectively. Under these conditions, the resulting  $L^2$  approximation errors achieve the optimal rates of order  $J_n^{-r}$  and  $K_n^{-s/p}$ , respectively. Assumption 4 ensures that the eigenvalues of the B-spline Gram matrix scale with  $J_n^{-1}$ , which can make the  $L^2$  norm of  $w(y)$  comparable to the Euclidean norm of its coefficients and thus allow effective control of function-level errors. Assumption 5 constrains the growth rates of  $J_n$  and  $K_n$  relative to the sample sizes, ensuring that the estimation error terms vanish asymptotically. Finally, Assumption 6 requires that  $\mathbf{U}$ ,  $\mathbf{V}^\top \mathbf{U}^{-1} \mathbf{V}$ , and their ridge-regularized versions remain uniformly positive definite, which can guarantee the existence of required matrix inverses and ensure that the estimator is unique and numerically stable.

**Theorem 2** *Under Assumptions 2–6, the estimator proposed in Section 2.2.1 satisfies*

$$\|\widehat{w} - w_0\|_{L^2}^2 = O_p \left( J_n^{-2r} + K_n^{-2s/p} + \frac{K_n J_n \log n}{n_P} + \frac{K_n \log n}{n_Q} + \delta_n^2 + \rho_n^2 \right),$$

where  $\|\cdot\|_{L^2}^2 := \int (\cdot)^2 dy$  denotes the squared  $L^2$ -distance;  $J_n$ ,  $K_n$  are the numbers of B-spline and Gaussian basis functions;  $r$ ,  $s$  denote smoothness levels;  $p$  is the covariate dimension; and  $\delta_n$ ,  $\rho_n$  are regularization parameters.

The proof of Theorem 2 is provided in the supplementary material. Theorem 2 demonstrates that, with appropriately chosen  $J_n$ ,  $K_n$ ,  $\delta_n$ , and  $\rho_n$ , and sufficiently large sample sizes, the estimation error  $\|\widehat{w} - w_0\|_{L^2}^2$  converges to zero at an explicit rate and becomes asymptotically negligible. For instance, assuming  $n_P \asymp n_Q$ , choosing  $J_n \asymp n_P^{1/(2r+1)}$ ,  $K_n \asymp n_Q^{p/(2s+p)}$ ,  $\delta_n \asymp \sqrt{(\log n_P)/n_P}$ , and  $\rho_n \asymp \sqrt{(\log n_Q)/n_Q}$ , the convergence rate becomes

$$O_p \left( n_P^{-r/(2r+1)} + n_Q^{-s/(2s+p)} \right),$$

which matches the minimax-optimal rates under the Sobolev–B-spline and Sobolev–Gaussian approximation frameworks, up to logarithmic factors. By combining Theorems 1 and 2, we conclude that the coverage probability of the CPUTS prediction set converges to the nominal

level  $1 - \alpha$  as the sample sizes tend to infinity.

## 4 Simulation Study

In this section, we investigate the finite-sample performance of the CPUTS method (Sections 2.3 and 2.2) through simulation studies conducted under both labeled-target and unlabeled-target scenarios. The experimental settings are detailed below.

To capture different forms of target shift, we consider two settings: (i) a **location shift**, with  $Y^P \sim N(0, 1)$  and  $Y^Q \sim N(1, 1)$ ; and (ii) a **location–scale shift**, with  $Y^P \sim N(0, 1.5^2)$  and  $Y^Q \sim N(1, 0.5^2)$ . Given  $Y$ , the covariate  $X$  is generated from (i) the **linear model**  $X = Y + \varepsilon$  and (ii) the **nonlinear model**  $X = U + \varepsilon$  with  $U \sim \log \text{Normal}(Y, 1)$ , where  $\varepsilon$  is drawn from a standardized skew-normal distribution with shape parameter 15. These mechanisms are applied to generate both  $X^P$  and  $X^Q$  from their respective  $Y^P$  and  $Y^Q$ . We generate  $n_P$  source samples  $(X^P, Y^P)$  and  $n_Q$  target samples  $(X^Q, Y^Q)$ , among which  $n_0 = 1000$  target samples are unlabeled and the remaining  $n_Q^{\text{lab}} = n_Q - n_0$  are labeled.

For weight estimation, we use cubic B-spline basis functions ( $d = 3$ ) for the response, with the number of basis functions set to  $J_n = 4.5n_{P,\text{tr}}^{1/5}$ , and Gaussian radial basis functions for the covariates, with  $K_n = n_{P,\text{tr}}^{1/5}$ , where  $n_{P,\text{tr}}$  denotes the size of the training data in  $P$ . Both  $J_n$  and  $K_n$  are constrained to the range  $[5, 25]$ . A common bandwidth  $\sigma_k \equiv \sigma$  is determined by Silverman’s rule of thumb,  $\sigma = 1.06 \min\{\widehat{\sigma}_X, \widehat{\text{IQR}}_X/1.349\} n_{P,\text{tr}}^{-1/5}$ , where  $\widehat{\sigma}_X$  and  $\widehat{\text{IQR}}_X$  denote the sample standard deviation and the interquartile range of the covariates. Small ridge penalties are applied, with  $\delta_n, \rho_n \in [10^{-6}, 10^{-4}]$ . For conditional density estimation, we employ linear quantile regression to estimate the quantile process. The numbers of quantile levels are set to  $\kappa^P = 2n_{P,\text{tr}}^{1/3}$  and  $\kappa^Q = 2n_{Q,\text{tr}}^{1/3}$  for the  $P$  and  $Q$  distributions, respectively, where  $n_{Q,\text{tr}}$  denotes the size of the training data in  $Q$ , with both constrained to the range  $[9, 25]$ . The corresponding quantile levels are then given by  $\tau_j^P = j/(\kappa^P + 1)$ ,  $j = 1, \dots, \kappa^P$ , and  $\tau_j^Q = j/(\kappa^Q + 1)$ ,  $j = 1, \dots, \kappa^Q$ . The bandwidth  $h_n$  is chosen according to the Hall–Sheather rule, as implemented in the *bandwidth.rq* function of the *quantreg* package, which has convergence rate  $O(n^{-1/3})$ .

To evaluate the performance of CPUTS under unlabeled target scenarios ( $n_Q^{\text{lab}} = 0$ ), we compare it with the classical conformal prediction method based on source  $P$  samples, referred to as CP-P, implemented using the *conformal.pred.split* function from the *conformalInference* R package. We compute coverage probabilities and interval lengths across different source sample sizes  $n_P$ , with a fixed total target sample size of  $n_Q = 1000$ . The results are averaged over 1000 replications, each based on 300 test points. Tables 1 and 2 report the results under the location-shift and location-scale-shift settings, respectively, and Figure 3 illustrates an example line plot for the location-shift nonlinear model. The CP-P method does not yield valid coverage, often resulting in under- or over-coverage, because directly using source  $P$  data to predict the  $Q$  distribution without adjustment introduces bias. In contrast, our CPUTS method generally achieves accurate coverage, and the interval length noticeably decreases as  $n_P$  increases.

Table 1: Coverage probability (CovP, %) and average length (AL, with standard error, SE) of 90% conformal prediction intervals across two models, with varying source sample sizes  $n_P$  and a total target sample size of  $n_Q = 1000$ . Results are averaged over 300 test points and 1000 replications, under the unlabeled target scenario ( $n_Q^{\text{lab}} = 0$ ) with a location shift.

$n_P$	CPUTS		CP-P	
	CovP	AL (SE)	CovP	AL (SE)
<i>Linear model</i>				
500	<b>90.8</b>	2.540 (0.010)	81.2	2.330 (0.004)
1000	<b>90.2</b>	2.317 (0.006)	80.9	2.318 (0.003)
2000	<b>89.9</b>	2.232 (0.003)	80.9	2.311 (0.002)
3000	<b>89.8</b>	2.212 (0.003)	80.6	2.309 (0.002)
4000	<b>89.6</b>	2.196 (0.002)	80.6	2.309 (0.002)
<i>Nonlinear model</i>				
500	<b>91.0</b>	2.487 (0.010)	81.2	2.330 (0.004)
1000	<b>90.3</b>	2.301 (0.005)	80.9	2.318 (0.003)
2000	<b>90.0</b>	2.236 (0.003)	80.9	2.311 (0.002)
3000	<b>89.9</b>	2.220 (0.003)	80.6	2.309 (0.002)
4000	<b>89.7</b>	2.210 (0.002)	80.6	2.309 (0.002)

CPUTS: Proposed method; CP-P: Conformal prediction using only  $P$ -distribution samples.

Next, to evaluate CPUTS under labeled target scenarios ( $n_Q^{\text{lab}} > 0$ ), we compare it with two classical conformal prediction methods: CP-P, which uses source  $P$  samples, and CP-Q, which uses labeled target  $Q$  samples. Tables 3 and 4 report the mean coverage probability

Table 2: Coverage probability (CovP, %) and average length (AL, with standard error, SE) of 90% conformal prediction intervals across two models, with varying source sample sizes  $n_P$  and a total target sample size of  $n_Q = 1000$ . Results are averaged over 300 test points and 1000 replications, under the unlabeled target scenario ( $n_Q^{\text{lab}} = 0$ ) with a location-scale shift.

$n_P$	CPUTS		CP-P	
	CovP	AL (SE)	CovP	AL (SE)
<i>Linear model</i>				
500	<b>91.2</b>	1.663 (0.008)	95.3	2.702 (0.005)
1000	<b>90.5</b>	1.549 (0.006)	95.3	2.683 (0.003)
2000	<b>90.5</b>	1.494 (0.005)	95.4	2.676 (0.002)
3000	<b>90.6</b>	1.481 (0.005)	95.5	2.674 (0.002)
4000	<b>90.5</b>	1.462 (0.005)	95.4	2.672 (0.002)
<i>Nonlinear model</i>				
500	<b>93.5</b>	2.388 (0.027)	98.8	4.365 (0.010)
1000	<b>91.9</b>	2.036 (0.017)	99.2	4.379 (0.008)
2000	<b>90.8</b>	1.855 (0.015)	99.3	4.402 (0.006)
3000	<b>90.5</b>	1.789 (0.013)	99.4	4.438 (0.006)
4000	<b>90.2</b>	1.754 (0.013)	99.5	4.456 (0.005)

CPUTS: Proposed method; CP-P: Conformal prediction using only  $P$ -distribution samples.

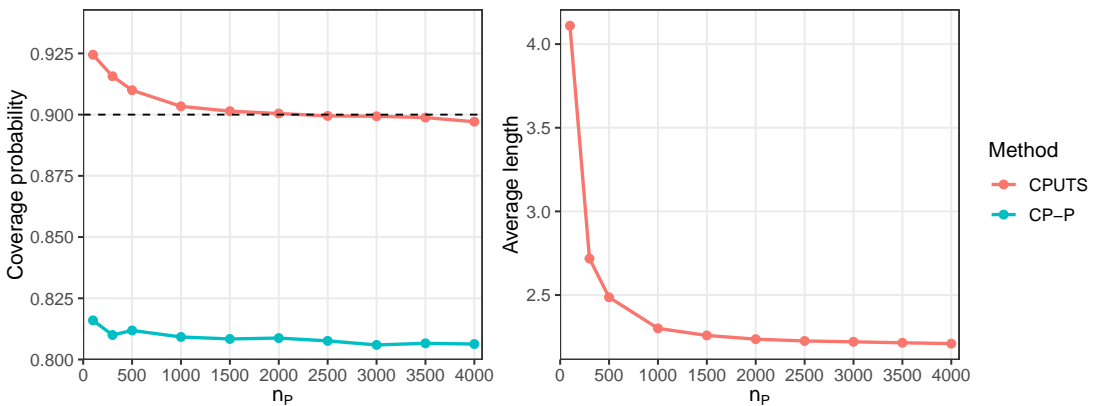


Figure 3: Coverage probability and average length of 90% conformal prediction intervals under a nonlinear model, with varying source sample sizes  $n_P$  and a total target sample size of  $n_Q = 1000$ , in the unlabeled target scenario with a location shift.

and interval length for varying  $n_Q^{\text{lab}}$ , with  $n_P = 2000$  and  $n_Q = 1000 + n_Q^{\text{lab}}$ . The two tables correspond to the location-shift and location-scale-shift settings, respectively. Although CP-Q achieves valid coverage, its intervals are wider than those of CPUTS, particularly when  $n_Q^{\text{lab}}$  is small. Under comparable coverage results, CPUTS reduces interval length by up to 48%.

Table 3: Coverage probability (CovP, %) and average length (AL, with standard error, SE) of 90% conformal prediction intervals across two models, with a fixed source sample size of  $n_P = 2000$  and varying target sample sizes  $n_Q = 1000 + n_Q^{\text{lab}}$ . Results are averaged over 300 test points and 1000 replications under the labeled target scenario with a location shift.

$n_Q^{\text{lab}}$	CPUTS		CP-P		CP-Q	
	CovP	AL (SE)	CovP	AL (SE)	CovP	AL (SE)
<i>Linear model</i>						
20	<b>90.0</b>	<b>2.383</b> (0.006)	80.9	2.309 (0.002)	90.7	2.970 (0.030)
50	<b>89.8</b>	<b>2.301</b> (0.005)	80.7	2.309 (0.002)	92.4	2.778 (0.019)
100	<b>89.9</b>	<b>2.269</b> (0.004)	80.7	2.310 (0.002)	90.2	2.427 (0.010)
300	<b>89.9</b>	<b>2.231</b> (0.004)	80.8	2.313 (0.002)	90.1	2.346 (0.006)
500	<b>89.9</b>	<b>2.220</b> (0.004)	80.8	2.312 (0.002)	90.1	2.330 (0.004)
<i>Nonlinear model</i>						
20	<b>89.9</b>	<b>2.968</b> (0.009)	78.4	2.936 (0.003)	91.0	5.748 (0.230)
50	<b>90.1</b>	<b>2.824</b> (0.006)	78.4	2.936 (0.003)	92.5	3.807 (0.068)
100	<b>90.3</b>	<b>2.809</b> (0.006)	78.4	2.936 (0.003)	90.1	3.025 (0.014)
300	<b>90.3</b>	<b>2.796</b> (0.006)	78.5	2.934 (0.003)	89.9	2.925 (0.007)
500	<b>90.2</b>	<b>2.787</b> (0.005)	78.2	2.934 (0.003)	90.0	2.920 (0.006)

CPUTS: Proposed method; CP-Q: Conformal prediction using only  $Q$ -distribution samples;  
CP-P: Conformal prediction using only  $P$ -distribution samples.

## 5 Data Application

To evaluate the real-world performance of our proposed method, we analyze the Medical Information Mart for Intensive Care III (MIMIC-III), a freely available database developed by the MIT Laboratory for Computational Physiology (<https://doi.org/10.13026/C2XW26>), as originally documented in [Johnson et al. \[2016\]](#). MIMIC-III contains health data from over 40,000 patients admitted to critical care units at Beth Israel Deaconess Medical Center between 2001 and 2012, including demographics, lab results, and vital signs. To predict a

Table 4: Coverage probability (CovP, %) and average length (AL, with standard error, SE) of 90% conformal prediction intervals across two models, with a fixed source sample size of  $n_P = 2000$  and varying target sample sizes  $n_Q = 1000 + n_Q^{\text{lab}}$ . Results are averaged over 300 test points and 1000 replications under the labeled target scenario with a location-scale shift.

$n_Q^{\text{lab}}$	CPUTS		CP-P		CP-Q	
	CovP	AL (SE)	CovP	AL (SE)	CovP	AL (SE)
<i>Linear model</i>						
20	<b>90.2</b>	<b>1.542</b> (0.006)	95.4	2.675 (0.003)	90.8	1.879 (0.019)
50	<b>90.2</b>	<b>1.515</b> (0.005)	95.4	2.676 (0.003)	92.4	1.745 (0.011)
100	<b>90.2</b>	<b>1.496</b> (0.005)	95.4	2.676 (0.003)	90.3	1.544 (0.006)
300	<b>90.2</b>	<b>1.484</b> (0.005)	95.5	2.678 (0.003)	90.2	1.497 (0.003)
500	<b>90.2</b>	1.486 (0.005)	95.5	2.677 (0.002)	90.0	1.483 (0.003)
<i>Nonlinear model</i>						
20	<b>90.6</b>	<b>1.857</b> (0.014)	99.3	4.402 (0.006)	91.0	2.356 (0.056)
50	<b>90.6</b>	<b>1.823</b> (0.015)	99.3	4.405 (0.006)	92.3	1.915 (0.019)
100	<b>90.6</b>	1.797 (0.015)	99.3	4.407 (0.006)	90.2	1.632 (0.007)
300	<b>90.8</b>	1.795 (0.015)	99.3	4.405 (0.006)	90.0	1.575 (0.004)
500	<b>90.6</b>	1.777 (0.014)	99.3	4.407 (0.006)	90.0	1.568 (0.003)

CPUTS: Proposed method; CP-Q: Conformal prediction using only  $Q$ -distribution samples;

CP-P: Conformal prediction using only  $P$ -distribution samples.

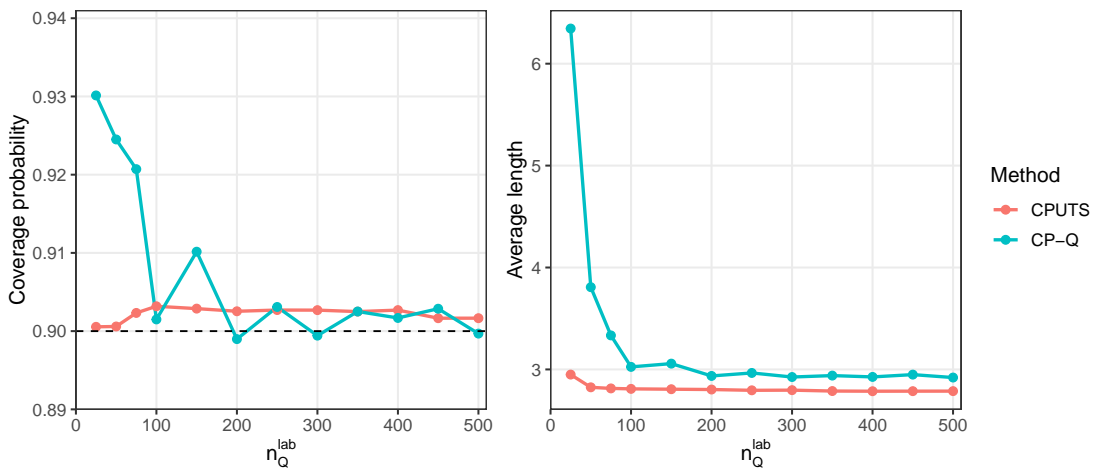


Figure 4: Coverage probability and average length of 90% conformal prediction intervals under a nonlinear model, with a source sample size of  $n_P = 2000$  and varying target sample sizes  $n_Q^{\text{lab}}$  in the labeled target scenario with a location shift.

patient's condition during their ICU stay and assess the extent of organ dysfunction or failure, we use the Sequential Organ Failure Assessment (SOFA) score as the response  $Y$ . The SOFA score consists of six components, each representing the function of a specific organ system: respiratory, cardiovascular, hepatic, coagulation, renal, and neurological. The total score ranges from 0 (best) to 24 (worst). Following [Lee et al. \[2025\]](#), we select covariates based on two criteria: an absolute correlation with the outcome  $Y$  greater than 0.2, and a missing rate less than 1%. As a result, we selected 16 covariates, including 6 vital signs (such as blood pressure, respiratory rate, oxygen saturation, and body temperature) and 10 lab tests (such as glucose, urea nitrogen, platelets, red blood cell count, and hematocrit). Following the data cleaning and preprocessing steps described in [Lee et al. \[2025\]](#), we obtained a total of  $n = 14,080$  records.

To investigate potential target shift across insurance types, we define the source population  $P$  as patients with private, government, or self-pay insurance ( $n_P = 9,580$ ), and the target population  $Q$  as those covered by Medicaid or Medicare ( $n_Q = 4,500$ ). Through the Kolmogorov-Smirnov test for distributional equality (p-value  $< 10^{-15}$ ), we found a significant difference in the marginal distribution of  $Y$  between  $P$  and  $Q$ , indicating that  $p(y) \neq q(y)$ . To assess whether  $p(\mathbf{x} \mid y) = q(\mathbf{x} \mid y)$ , we use the invariant environment prediction test [[Heinze-Deml et al., 2018](#)] from the R package *CondIndTests* to test the conditional independence between each covariate  $\mathbf{x}$  and insurance type given  $Y$ . The obtained p-values, ranging from 0.12 to 0.79, indicate no significant difference between  $p(\mathbf{x} \mid y)$  and  $q(\mathbf{x} \mid y)$ , thereby supporting the assumption that target shift holds in our setting. We observe that the five racial groups—White ( $n = 10,804$ ), Black ( $n = 1,538$ ), Asian ( $n = 410$ ), Hispanic ( $n = 767$ ), and Other ( $n = 561$ )—have varying effects on the outcome  $Y$ . However, race is not suitable as a covariate because the target shift assumption  $p(\mathbf{x}|y) = q(\mathbf{x}|y)$  does not hold: the Cochran–Mantel–Haenszel test for conditional independence (p-value  $< 10^{-15}$ ) strongly rejects the null hypothesis that race and insurance type are conditionally independent given  $Y$ . Therefore, we perform predictions separately for each of the five racial groups. For each group, we applied the same conditional independence test as above and confirmed that the

target shift assumption holds.

Table 5: Coverage probability (CovP, %) and interval length (AL, with standard error, SE) of 90% conformal prediction intervals across racial groups, averaged over all leave-one-out samples.

Race	Method	Sample Size	CovP%	AL (SE)	$ \text{CPUTS}  <  \text{CP-Q} $
White	CPUTS	–	<b>0.901</b>	<b>7.349(0.060)</b>	68.0%
	CP-Q	3098	0.899	8.081(0.007)	–
	CP-P	7706	0.870	7.174(0.003)	–
Black	CPUTS	–	<b>0.892</b>	<b>7.383(0.124)</b>	70.7%
	CP-Q	738	0.921	8.176(0.029)	–
	CP-P	800	0.878	7.464(0.020)	–
Asian	CPUTS	–	<b>0.915</b>	<b>7.595(0.276)</b>	94.4%
	CP-Q	141	0.915	13.286(0.436)	–
	CP-P	269	0.887	7.503(0.081)	–
Hispanic	CPUTS	–	<b>0.893</b>	<b>7.906(0.188)</b>	84.8%
	CP-Q	356	0.893	10.399(0.109)	–
	CP-P	411	0.854	7.734(0.039)	–
Other	CPUTS	–	<b>0.905</b>	<b>6.952(0.220)</b>	79.8%
	CP-Q	167	0.857	9.427(0.187)	–
	CP-P	394	0.833	7.986(0.065)	–

CPUTS: Proposed method; CP-Q: Conformal prediction using only  $Q$ -distribution samples; CP-P: Conformal prediction using only  $P$ -distribution samples;  $|\text{CPUTS}| < |\text{CP-Q}|$ : Proportion of instances in which the prediction interval length from CPUTS is shorter than that from CP-Q.

We apply our semi-supervised method, CPUTS, to predict SOFA scores for the target patients—those covered by Medicaid and Medicare—in the labeled target scenario, and compare it with two classical conformal prediction methods, CP-Q and CP-P, as described in Section 4. To obtain stable quantile estimates for the ordinal outcome  $Y$ , we add a tiny random noise sampled from  $N(0, 10^{-12})$  before computing the quantiles, which has negligible impact on the resulting prediction intervals. Standard approaches to ordinal quantile estimation can be found in [Machado and Silva \[2005\]](#) and [Hong and He \[2010\]](#). Following the parameter settings detailed in Section 4, we obtain the results summarized in Table 5, which show predictive performance across the different racial groups, averaged over all test points from leave-one-out cross-validation. Both CPUTS and CP-Q achieve valid coverage probabilities, whereas CP-P exhibits biased coverage due to distributional shift between the training and test data. Moreover, CPUTS consistently yields shorter prediction intervals than CP-Q, particularly when the number of  $Q$ -samples is limited. For example, in the Asian subgroup, CPUTS produces shorter intervals for 94.4% of test points compared with

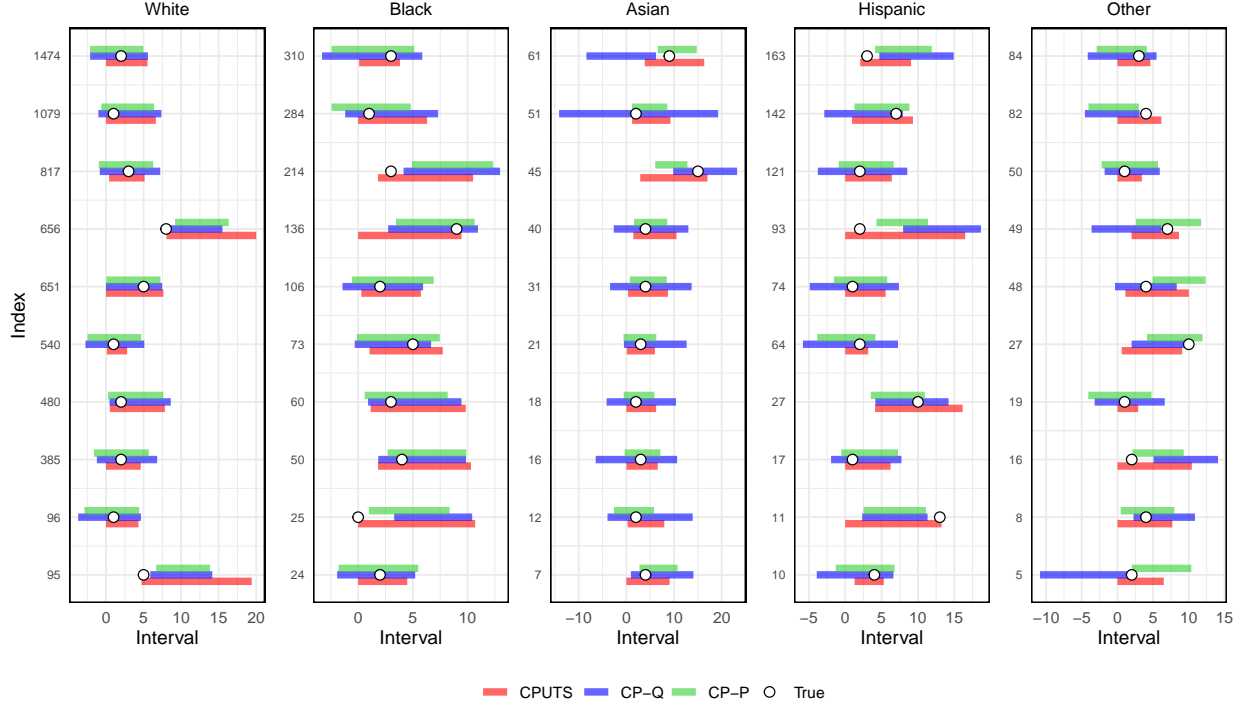


Figure 5: Comparison of 90% prediction intervals from the CPUTS, CP-Q, and CP-P methods for 15 selected subjects (indices shown on the vertical axis) across five datasets.

CP-Q, highlighting the effectiveness of the proposed method. We also show the prediction intervals for 15 selected patients from each racial subgroup in Figure 5, which support the same conclusion.

## 6 Conclusion

In this work, we propose CPUTS to address the target shift problem between source and target data, covering two cases: when the target distribution has no labels or only a few labeled samples. The method only guarantees asymptotic marginal coverage in Theorem 1, leaving room for improvement. First, the coverage can be improved by defining local subgroups based on specific features, which would allow for subgroup-level or conditional coverage guarantees. Second, the coverage depends on the accuracy of the weight estimation. Although this error can be controlled, better properties may be achievable—such as the doubly robust property, where accurate estimation of either the weights or the conditional

density would be sufficient. In addition, our current framework uses a single source dataset to improve prediction for the target data. In practice, however, multiple source datasets with different distributions are often available, and integrating them to enhance predictive efficiency is an interesting direction for future work.

## References

A. Alexandari, A. Kundaje, and A. Shrikumar. Maximum likelihood with bias-corrected calibration is hard-to-beat at label shift adaptation. In *International Conference on Machine Learning*, pages 222–232. PMLR, 2020.

S. Athey, J. Tibshirani, and S. Wager. Generalized random forests. *The Annals of Statistics*, 47(2):1148–1178, 2019.

K. Azizzadenesheli, A. Liu, F. Yang, and A. Anandkumar. Regularized learning for domain adaptation under label shifts. *arXiv preprint arXiv:1903.09734*, 2019.

R. F. Barber, E. J. Candes, A. Ramdas, and R. J. Tibshirani. Conformal prediction beyond exchangeability. *The Annals of Statistics*, 51(2):816–845, 2023.

M. D. Buhmann. Radial basis functions. *Acta numerica*, 9:1–38, 2000.

E. Candes, L. Lei, and Z. Ren. Conformalized survival analysis. *Journal of the Royal Statistical Society Series B: Statistical Methodology*, 85(1):24–45, 2023.

M. Cauchois, S. Gupta, A. Ali, and J. C. Duchi. Robust validation: Confident predictions even when distributions shift. *Journal of the American Statistical Association*, 119(548):3033–3044, 2024.

Y. S. Chan and H. T. Ng. Word sense disambiguation with distribution estimation. In *IJCAI*, volume 5, pages 1010–5, 2005.

R. Dunn, L. Wasserman, and A. Ramdas. Distribution-free prediction sets for two-layer hierarchical models. *Journal of the American Statistical Association*, 118(544):2491–2502, 2023.

I. Gibbs and E. J. Candès. Adaptive conformal inference under distribution shift. *Advances in Neural Information Processing Systems*, 34:1660–1672, 2021.

I. Gibbs and E. J. Candès. Conformal inference for online prediction with arbitrary distribution shifts. *Journal of Machine Learning Research*, 25(162):1–36, 2024.

J. Guo, M. Gong, T. Liu, K. Zhang, and D. Tao. Ltf: A label transformation framework for correcting label shift. In *International Conference on Machine Learning*, pages 3843–3853. PMLR, 2020.

T. Hastie, R. Tibshirani, J. H. Friedman, and J. H. Friedman. *The elements of statistical learning: data mining, inference, and prediction*, volume 2. Springer, 2009.

C. Heinze-Deml, J. Peters, and N. Meinshausen. Invariant causal prediction for nonlinear models. *Journal of Causal Inference*, 6(2):20170016, 2018.

H. G. Hong and X. He. Prediction of functional status for the elderly based on a new ordinal regression model. *Journal of the American Statistical Association*, 105(491):930–941, 2010.

X. Hu and J. Lei. A two-sample conditional distribution test using conformal prediction and weighted rank sum. *Journal of the American Statistical Association*, 119(546):1136–1154, 2024.

R. Izbicki, G. Shimizu, and R. B. Stern. Cd-split and hpd-split: Efficient conformal regions in high dimensions. *Journal of Machine Learning Research*, 23(87):1–32, 2022.

A. E. Johnson, T. J. Pollard, L. Shen, L.-w. H. Lehman, M. Feng, M. Ghassemi, B. Moody, P. Szolovits, L. Anthony Celi, and R. G. Mark. Mimic-iii, a freely accessible critical care database. *Scientific data*, 3(1):1–9, 2016.

R. Koenker. *Quantile regression*, volume 38. Cambridge university press, 2005.

S.-h. Lee, Y. Ma, and J. Zhao. Doubly flexible estimation under label shift. *Journal of the American Statistical Association*, 120(549):278–290, 2025.

J. Lei, J. Robins, and L. Wasserman. Distribution-free prediction sets. *Journal of the American Statistical Association*, 108(501):278–287, 2013.

J. Lei, M. G’Sell, A. Rinaldo, R. J. Tibshirani, and L. Wasserman. Distribution-free predictive inference for regression. *Journal of the American Statistical Association*, 113(523):1094–1111, 2018.

L. Lei and E. J. Candès. Conformal inference of counterfactuals and individual treatment effects. *Journal of the Royal Statistical Society Series B: Statistical Methodology*, 83(5):911–938, 2021.

Z. Lipton, Y.-X. Wang, and A. Smola. Detecting and correcting for label shift with black box predictors. In *International conference on machine learning*, pages 3122–3130. PMLR, 2018.

J. A. F. Machado and J. M. C. S. Silva. Quantiles for counts. *Journal of the American Statistical Association*, 100(472):1226–1237, 2005.

T. D. Nguyen, M. Christoffel, and M. Sugiyama. Continuous target shift adaptation in supervised learning. In *Asian Conference on Machine Learning*, pages 285–300. PMLR, 2016.

M. D. Plessis and M. Sugiyama. Semi-supervised learning of class balance under class-prior change by distribution matching. *Neural Networks*, 50:110–119, 2014.

A. Podkopaev and A. Ramdas. Distribution-free uncertainty quantification for classification under label shift. In *Uncertainty in artificial intelligence*, pages 844–853. PMLR, 2021.

M. Saerens, P. Latinne, and C. Decaestecker. Adjusting the outputs of a classifier to new a priori probabilities: a simple procedure. *Neural computation*, 14(1):21–41, 2002.

L. Schumaker. *Spline functions: basic theory*. Cambridge university press, 2007.

G. Shafer and V. Vovk. A tutorial on conformal prediction. *Journal of Machine Learning Research*, 9(3), 2008.

M. M. Siddiqui. Distribution of quantiles in samples from a bivariate population. *J. Res. Nat. Bur. Standards B*, 64:145–150, 1960.

R. J. Tibshirani, R. Foygel Barber, E. Candes, and A. Ramdas. Conformal prediction under covariate shift. *Advances in neural information processing systems*, 32, 2019.

V. Vovk, A. Gammerman, and G. Shafer. *Algorithmic learning in a random world*, volume 29. Springer, 2005.

K. Zhang, B. Schölkopf, K. Muandet, and Z. Wang. Domain adaptation under target and conditional shift. In *International conference on machine learning*, pages 819–827. Pmlr, 2013.